

Statistical analysis of drill pipe failures of strength groups S-135 and G-105

Analiza statystyczna uszkodzeń rur wiertniczych z grup wytrzymałości S-135 i G-105

Yevstakhii Kryzhanivskiyi, Oleg Vytyaz, Roman Hrabovskiyi, Volodymyr Tyrlych

Ivano-Frankivsk National Technical University of Oil and Gas, Ukraine

ABSTRACT: The characteristic types of operational defects that can form on the inner or outer surface of drill pipes of strength groups S-135 and G-105 (according to API Spec 5DP) are described using the results of technical diagnostics from drilling wells in the Dnipro-Donetsk gas and oil region. In 2018 and 2019, the Ukrburgaz Drilling Department rejected 81 drill pipes of strength group S-135 and 89 drill pipes of strength group G-105 when drilling wells to a depth of 4000 to 6000 m. A statistical evaluation of the operational defects detected during deep drilling of wells (4000–6000 m) was carried out. Potentially dangerous areas were identified: in the drilling pipe upset zone and along the length of the drill string end drill pipes lifetime has been taken into account. It is recommended during defectoscopy of drill string pipes of the selected strength groups to pay close attention to the sections of pipes of strength group S-135 from the end of the coupling or nipple, in the range of 0.45 m to 0.57 m, and for sections of pipes of strength group G-105, in the range of 0.55 m to 0.63 m. In addition, given the depth of drilling (L_{max}), when performing diagnostics on drill pipes, special attention should be paid to sections with the most likely defect (L_f) along the length of the drill string. In particular, taking into account the relative length (L_f/L_{max}) of the drill string, for pipes of strength groups S-135 and G-105, segments in the ranges of 0.34 to 0.47 and 0.43 to 0.52, respectively, were identified as having the highest probability of operational defects. The peculiarities of the influence of a drill pipe operating lifespan depending on the strength group were established. In particular, during the long-term deepening of drill pipes in strength group S-135, three stages of drilling were distinguished: Stage I – running-in (from start-up to 2000 hours); Stage II – stable work (2000 to 7000 hours); and Stage III – accelerated destruction (7000 hours and longer). It was found that during defectoscopy of the pipe, special attention should be paid to the drill pipe, the service life of which is 602–998 hours in the first stage, from 3348 to 5344 hours in the second stage, and from 8942 to 10584 hours in the third stage, because these periods carry the greatest probability of originating an inadmissible defect. For long-term drilling works with pipes of strength group G-105, two stages of drilling were distinguished: the first stage, of stable work (up to 6000 hours), and the second stage, of accelerated destruction (6000 hours and longer). It was found that during defectoscopy of the pipe, special attention should be paid to the drill pipe, the service life of which is from 2692 to 3736 hours in the first stage and from 8744 to 10983 hours in the second stage, because these periods demonstrate the greatest probability of an inadmissible defect.

Key words: drill pipes, drill strings, operational defects.

STRESZCZENIE: W artykule opisano charakterystyczne rodzaje wad eksploatacyjnych powstałych na wewnętrznej lub zewnętrznej powierzchni rur wiertniczych z grup wytrzymałości S-135 i G-105 (według API Spec 5DP). Wykorzystano wyniki diagnostyki technicznej podczas wiercenia odwiertów na terenie dniewrowsko-donieckiego regionu ropno-gazowego. W latach 2018–2019 Oddział Wiertniczy Ukrburgaz odrzucił 81 rur wiertniczych grupy wytrzymałości S-135 i 89 rur wiertniczych grupy wytrzymałości G-105 przy wierceniu odwiertów do głębokości od 4000 m do 6000 m. Przeprowadzono ocenę statystyczną wykrytych wad eksploatacyjnych powstałych podczas głębokich wierceń (4000–6000 m). Zidentyfikowano obszary potencjalnie niebezpieczne – w strefie uszkodzenia pojedynczych rur wiertniczych oraz na długości przewodu wiertniczego; uwzględniono czas użytkowania rur wiertniczych. Zaleca się, aby przy defektoskopii rur przewodu wiertniczego badanych grup wytrzymałościowych zwrócić szczególną uwagę na odcinki rur grupy wytrzymałości S-135 od końca złączki lub łącznika w zakresie od 0,45 m do 0,57 m, a dla odcinków rur z grupy wytrzymałości G-105 – w zakresie od 0,55 m do 0,63 m. Dodatkowo, ze względu na głębokość wiercenia (L_{max}), wzmożoną uwagę przy diagnozowaniu rur należy zwrócić na odcinki o najbardziej prawdopodobnej usterce (L_f) na całej długości przewodu wiertniczego. W szczególności dla rur z grup wytrzymałościowych S-135 i G-105, biorąc pod uwagę długość względną (L_f/L_{max}) przewodu wiertniczego, zidentyfikowano segmenty w zakresie odpowiednio od 0,34 do 0,47 oraz od 0,43 do 0,52, na których występuje najwyższe prawdopodobieństwo wystąpienia wady eksploatacyjnej. Ustalono osobliwości wpływu czasu użytkowania rur wiertniczych w zależności od grupy wytrzymałości. W szczególności podczas długotrwałego głębenia odwiertów przy użyciu rur wiertniczych grupy wytrzymałościowej S-135 wyróżniono trzy etapy wierceń: I etap – docieranie (od rozruchu do 2 tys. godzin); II etap – praca stabilna (od 2 tys. do 7 tys. godzin)

i III etap – przyspieszone niszczenie (powyżej 7 tys. godzin). Stwierdzono, że podczas defektoskopii rur wiertniczych należy zwrócić szczególną uwagę na czas trwania eksploatacji, który w pierwszym etapie wynosi odpowiednio od 602 do 998 godzin, w drugim – od 3348 do 5344 godzin, a w trzecim – od 8942 do 10 584 godzin, gdyż w tych okresach istnieje największe prawdopodobieństwo powstania wady niedopuszczalnej. Przy długotrwałych pracach wiertniczych rurami grupy wytrzymałości G-105 wyróżnia się dwa etapy wiercenia: pierwszy etap – praca stabilna (do 6 tys. godzin) i drugi etap – przyspieszone niszczenie (powyżej 6 tys. godzin). Stwierdzono, że podczas defektoskopii tych rur należy zwrócić szczególną uwagę na rury, których czas trwania eksploatacji w pierwszym etapie wynosi od 2692 do 3736 godzin, a w drugim etapie – od 8744 do 10 983 godzin, ponieważ w tych okresach istnieje największe prawdopodobieństwo wystąpienia wady niedopuszczalnej.

Słowa kluczowe: rury wiertnicze, przewody wiertnicze, wady eksploatacyjne.

Introduction

In Ukraine, the main prospects for the discovery of oil and gas fields at great depths today are found in the Dniepro-Donetsk depression. The high prospects of deep horizons in the Dniepro-Donetsk depression have been confirmed by the recent discoveries of gas condensate deposits at depths of about 6000 to 7000 m in the Semirenkivsky and Komyschnyansky fields. The peculiarities of the deep geological structure of oil and gas fields in the Dniepro-Donetsk depression include low angles of rock bedding, density and fracturing and weak reservoir properties. However, as practice shows (Information Bulletin for 2018; Information Bulletin for 2019), drilling at such depths leads to a significant increase in the number of accidents (Albdiry and Almensory, 2016); for example, in

the drilling interval of 2500 to 4500 m the number of failures increases 4.8 to 5 times, while in the range of 4500 to 5000 m it increases 9.8 times.

An analysis of more than 750 drill string (DS) accidents in the Iranian oil field (Zamani et al., 2016) revealed weaknesses in the drill pipes (DP) which were the origin (formation or initiation) of operational defects. In Ahmed et al. (2020), the destruction of a G-105 DP (127.0 × 9.20 mm) after 2367 hours of net drilling time to a depth of 8726 m was studied and a systematic analysis of the operating conditions and DP loading was conducted. According to the results, it was determined that the accidents were caused by drill pipe flushing or destruction due to corrosion/fatigue development of the crack. The stages of destruction were as follows: corrosion ulcers (Figure 1a) first appeared on the inner surface in the zone of stress con-

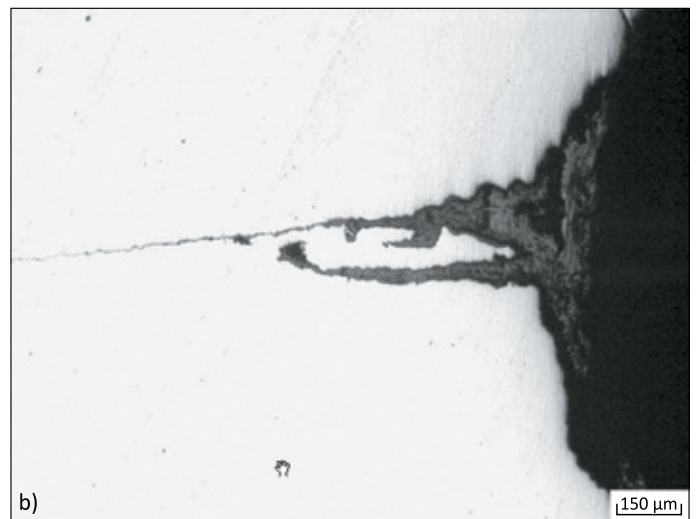
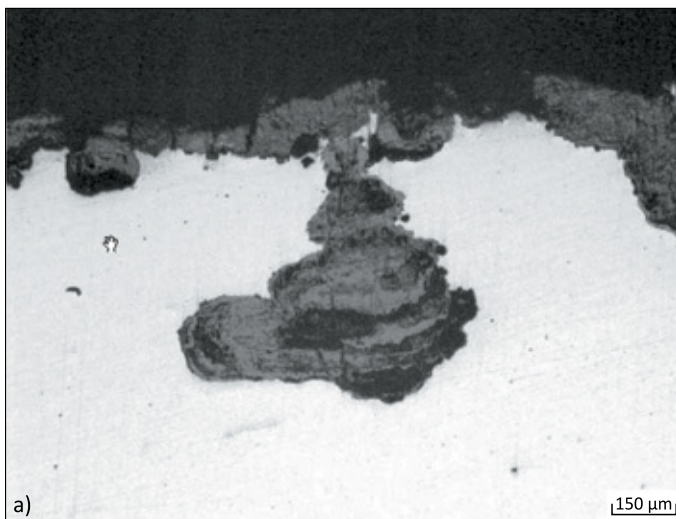


Figure 1. Morphology of corrosion ulcers on the inner surface of the flushing hole (a) and cracks arising from corrosion ulcers near the end of the internal narrowing (b), as well as flushing on the drill pipe (c) (Lu et al., 2005; Lukin et al., 2020)

Rysunek 1. Morfologia wżerów korozyjnych na wewnętrznej powierzchni wypłukanego otworu (a) oraz pęknięć powstałych w wyniku wżerów korozyjnych w rejonie zakończenia wewnętrznego przewężenia (b) oraz wypłukania na rurze płuczkowej (c) (Lu et al., 2005; Lukin et al., 2020)

centration in the drill pipe (Syrotyuk and Dmytrakh, 2014); then corrosion/fatigue cracks (Figure 1b) (Kryzhanivs'kyi et al., 2004, 2018; Vytyaz et al., 2020) appeared at the bottom of the corrosion ulcers develop forming flushing (Figure 1c); this eventually lead to the destruction of the pipe (Panasyuk et al., 2014) because the crack passing through the wall of the DP continues to develop in the transverse direction.

A significant number of theoretical studies have been devoted to the trouble-free operation of drill pipes and tools under

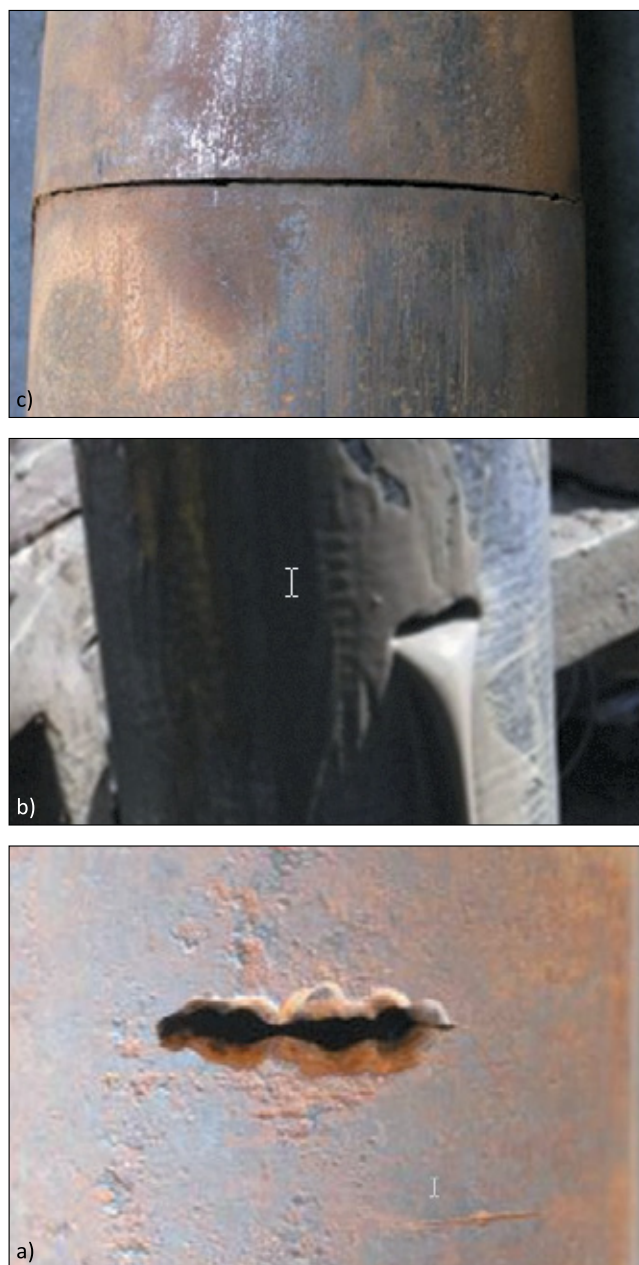


Figure 2. Typical operational defects of drill pipes of strength group S-135: flush – elliptical hole (a, b) (Zamani et al., 2016; Ahmed et al., 2020), flush slit – crack-like defect (c) (Guo et al., 2022)

Rysunek 2. Typowe wady eksploatacyjne rur płuczkowych grupy wytrzymałości S-135: wypłukanie – otwór eliptyczny (a, b) (Zamani et al., 2016; Ahmed et al., 2020), szczelina zlicowana – wada podobna do pęknięcia (c) (Guo et al., 2022)

extreme operating conditions (Moisyshyn and Levchuk, 2017; Ropyak et al., 2020; Bazaluk et al., 2021), the calculation of stresses in the threaded connections of the nipple with the coupling (Pryhorovska and Ropyak, 2019; Tutko et al., 2021) and the assessment of allowable loads on elongated underground structures (Kryzhanivs'kyi et al., 2004; Velychkovych et al., 2019).

Methods for predicting the lifespan of pipes operated long-term with through and surface cracks and corrosion defects are described in Hrabovs'kyi (2009), Kryzhanivs'kyi et al. (2013, 2015) and Tyrlych and Moisyshyn (2019). In particular, the role of the crack closure effect has been noted in the literature (Liu et al., 2004; Shats'kyi and Makoviichuk, 2009).

Electrochemical research methods are used to assess the degradation of pipe steel during operation. These methods can predict the resistance of steel to brittle fracture from changes in its electrochemical parameters (Zvirko et al., 2021).

Analyses of emergencies caused by the action of operating loads on DPs and the impact of flushing fluids during rotary drilling (Liu et al., 2016; Kryzhanivs'kyi et al., 2021; Guo et al., 2022) showed that such emergencies lead to flushing of DPs (Figure 2a) or DP breakage due to the formation and development of corrosion/fatigue cracks (Figure 2b).

In Kryzhanivs'kyi et al. (2021), an assessment of the breakage conditions from DPs of strength groups S-135 and G-105 were considered. It was demonstrated that the operation of the DS is determined by the conditions and duration of the load within its components, depending on the drilling trajectory. Therefore, it is relevant to statistically evaluate the potentially dangerous segments located along the length of the DP as elements of the DS. Other urgent scientific and technical problems are the statistical evaluation of potentially dangerous areas along the length of the DS and of the duration of drilling, which requires special attention in technical diagnostics.

The purpose of the work is to assess the potentially dangerous areas of DPs in strength groups S-135 and G-105 and of DSs which emerge when wells are deepened, using statistical data on emergency situations and approaches to mathematical statistics.

Analysis and characterisation of the defects that form on drill pipes during operation

It is known that nipples and couplings serve as potential sources of cracks in a DP (Albdiry and Almensory, 2016). The welding zone and the thickened part of a DP are critical places for the formation of operation defects, due to their geometry. Figures 3 and 4 show the radial flushes and fatigue cracks observed in the transition zone of a DP.

Thus, through fault operation defects detected in the process of diagnosing DP can be divided into two types, according to their shape (Lu et al., 2005; Lukin et al., 2020; Guo et al., 2022;). The first type is characterised by an ‘oval shape of the flushing hole’, as shown in Figures 1c, 2 and 3. At the same time, the flushing hole is thoroughly washed out by the flushing liquid, and the top of the developing crack becomes passive. An ‘oval through hole’ is usually formed, provided that the rate of crack propagation is rather slow. The second type is characterised by a through hole – ‘a flushing gap’. In this case, the width of the flushing hole is 0.5~5.0 mm. Further development of the crack occurs transversely to the critical size, which leads to failure of the drill pipe, as shown in Figures 2 and 3.

The fundamental difference, from the standpoint of fracture mechanics, between the two types of through defects – a narrow slit and a contact crack – was also noted in Shats’kyi and Dalyak (2002) and Dalyak and Shatskyi (2020).



Figure 3. Flushing hole and fatigue crack in internal failure (Zamani et al., 2016)

Rysunek 3. Wyplukany otwór i pęknięcie zmęczeniowe w przypadku uszkodzenia wewnętrznego (Zamani et al., 2016)



Figure 4. Flushing holes of the drill pipe in the transition zone (Liu et al., 2011)

Rysunek 4. Wyplukane otwory w rurach płuczkowych w strefie przejściowej (Liu et al., 2011)

Statistical analysis of the location of defects that form near the DP upset zone

During defectoscopy (Information Bulletin for 2018; Information Bulletin for 2019) on the wells of Ukrburgaz in 2018 and 2019, 81 DPs of strength group S-135 and 89 DPs of strength group G-105 were rejected when drilling wells to a depth (L_{max}) of 4000 to 6000 m. On the body of the DPs of strength group S-135 operated at a distance of up to 1 m from the coupling face or nipple, 15 inadmissible through transverse corrosion/fatigue cracks and 66 flushes were found; for pipes of strength group G-105 28 inadmissible through transverse corrosion/fatigue cracks and 61 flushes were detected. The depths at which these defects were formed (L_f) and the duration of their operation at the time of defectoscopy were also determined.

It is known that the area where pipes are upset is the most vulnerable site (Ahmed et al., 2020), as this is where the stresses acting on DPs are concentrated. This means that the accumulation of microcracking is more intensive. In addition, wedges and other equipment holding a DP have a destructive effect on the upset zone from the side clutch. Any scratch or dent on the surface of a pipe automatically becomes a stress concentrator and accelerates the accumulation of fatigue microcracks in the area.

The upset zone of the pipes under study, i.e. one-metre-long sections, was divided into a number of intervals, and the numbers of defects were grouped accordingly. The resulting variation series is presented in Table 1. A frequency diagram (Figure 5) and a histogram (Figure 6) were built for the distribution (Kalbfleisch and Prentice, 2011; Syrotyuk and Dmytrakh, 2014; Dmytrakh et al., 2018).

An assessment of a number of distributions was given (Table 1), determining the characteristic indicators (Table 2). Numerical (Table 3) and relative (Table 4) indicators of variation were determined. To characterise the resulting series, the indicators for the form of distribution and the degree of asymmetry were determined (Table 5).

Because $Ex/S_{Ex} < 3$, the deviation from the normal distribution for DT S-135 is considered insignificant. For DT,

Table 1. Data on failures (detected defects) in the upset zone, 2018–2019

Tabela 1. Dane o awariach (wykrytych wadach) w obszarze zaburzenia rur płuczkowych za lata 2018–2019

| Strength group | Length interval, L [m] | | | | | | | | | |
|----------------|--------------------------|---------|---------|---------|---------|---------|---------|---------|---------|---------|
| | 0.0–0.1 | 0.1–0.2 | 0.2–0.3 | 0.3–0.4 | 0.4–0.5 | 0.5–0.6 | 0.6–0.7 | 0.7–0.8 | 0.8–0.9 | 0.9–1.0 |
| | number, n | | | | | | | | | |
| S-135 | 8 | 0 | 1 | 8 | 9 | 31 | 19 | 2 | 1 | 2 |
| G-105 | 1 | 1 | 0 | 4 | 10 | 30 | 34 | 4 | 1 | 4 |

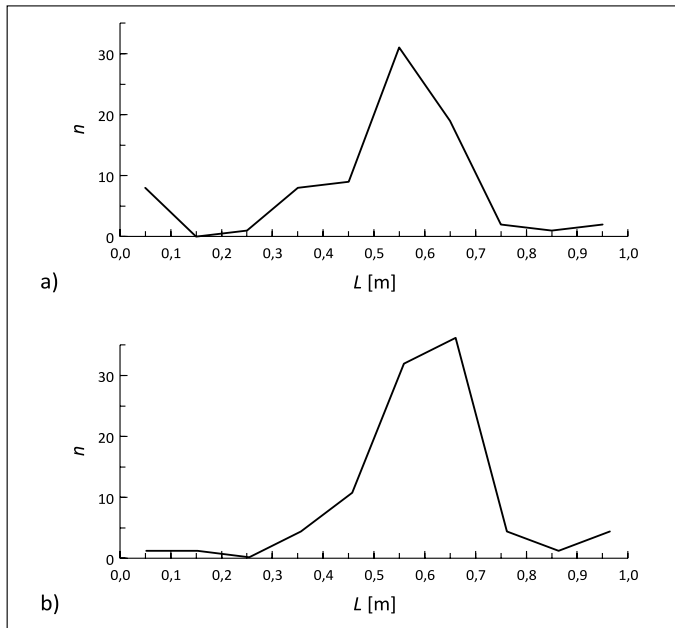


Figure 5. Frequency diagram: DP S-135 (a), DP G-105 (b)
Rysunek 5. Wykres częstotliwości: DP S-135 (a), DP G-105 (b)

G-105 $Ex/S_{Ex} > 3$, the deviation from the normal distribution is considered significant. An interval estimate of the centre of the general population was obtained. The confidence interval for the population mean was determined from the ratio

$$\left(\bar{x} - t_{\kappa p} \cdot \frac{s}{\sqrt{n}}; \bar{x} + t_{\kappa p} \cdot \frac{s}{\sqrt{n}} \right)$$

and the reliability interval was calculated for a sufficiently high value of reliability. The results of the calculations are presented in Table 6.

From an analysis of the calculations resulting from Table 6 (level of reliability $\gamma = 0.005$), corresponding to the highest probability of an operational defect, it can be concluded that when performing defectoscopy on DPs of strength group S-135,

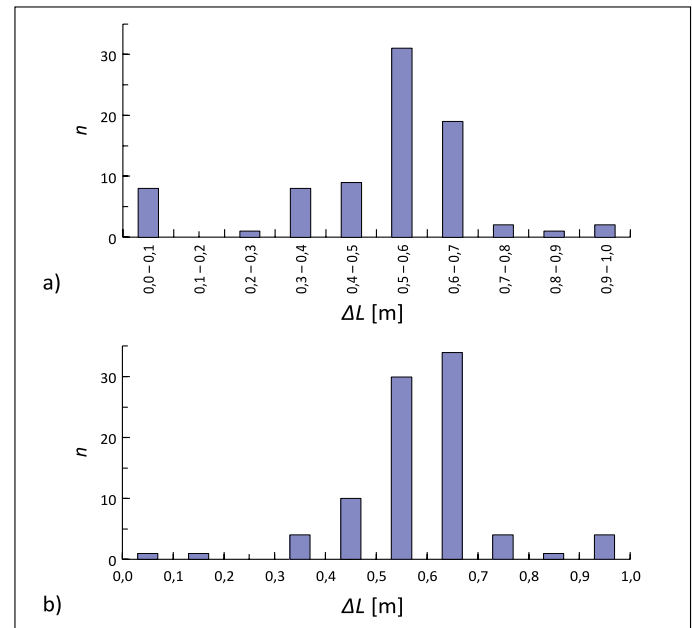


Figure 6. Histogram: DT S-135 (a), DT G-105 (b)
Rysunek 6. Histogram: DT S-135 (a), DT G-105 (b)

Table 2. Indicators for the statistical series of the distribution of the number of defects

Tabela 2. Wskaźniki charakteryzujące szeregi statystyczne rozkładu wykrytej liczby defektów

| Strength group | Selective average | Mode | Median |
|----------------|-------------------|--------------|--------------|
| S-135 | $\bar{x} = 0.508$ | $Mo = 0.565$ | $Me = 0.547$ |
| G-105 | $\bar{x} = 0.588$ | $Mo = 0.612$ | $Me = 0.595$ |

increased attention should be paid to the area in the range of 0.45 m to 0.57 m from the end (L), and that for defectoscopy of DPs of strength group G-105 increased attention should be paid to the area in the range of 0.55 m to 0.63 m from the end.

Table 3. Numerical indicators of variation

Tabela 3. Liczbowe wskaźniki zmienności

| Range of variability | Mean linear deviation | Dispersion | Corrected dispersion | Standard deviation | Estimation of standard deviation |
|----------------------|-----------------------|--------------|----------------------|--------------------|----------------------------------|
| Strength group S-135 | | | | | |
| $R = 1$ | $d = 0.141$ | $D = 0.375$ | $S^2 = 0.038$ | $\sigma = 0.194$ | $s = 0.195$ |
| Strength group G-105 | | | | | |
| $R = 1$ | $d = 0.1$ | $D = 0.0199$ | $S^2 = 0.201$ | $\sigma = 0.141$ | $s = 0.142$ |

Table 4. Relative indicators of variation

Tabela 4. Względne wskaźniki zmienności

| Strength group | Coefficient of variation | Relative linear deviation | Oscillation coefficient |
|----------------|--------------------------|---------------------------|-------------------------|
| | [%] | | |
| S-135 | $v = 38.12$ | $K_d = 27.75$ | $K_r = 196.84$ |
| G-105 | $v = 23.98$ | $K_d = 17.00$ | $K_r = 170.01$ |

Table 5. Indicators for the form of distribution and the degree of asymmetry

Tabela 5. Wskaźniki postaci rozkładu i stopnia asymetrii

| Instantaneous asymmetry coefficient | Mean-square error of asymmetry coefficient | Pearson's asymmetry structural coefficient | Kurtosis indicator (peakedness) | Mean-square error of kurtosis coefficient | Materiality of kurtosis |
|--|--|--|---------------------------------|---|-------------------------|
| Strength group S-135 | | | | | |
| $A_s = -0.887$ | $S_{A_s} = 0.579$ | $A_{sp} = -0.29^*$ | $Ex = 1.09^{**}$ | $S_{Ex} = 0.755$ | $Ex / S_{Ex} = 1.444$ |
| Strength group G-105 | | | | | |
| $A_s = -0.360$ | $S_{A_s} = 0.579$ | $A_{sp} = -0.16^*$ | $Ex = 3.07^{**}$ | $S_{Ex} = 0.755$ | $Ex / S_{Ex} = 4.068$ |
| * A negative sign indicates left asymmetry | | | | | |
| ** A positive sign indicates a peaked distribution | | | | | |

Table 6. Reliability intervals

Tabela 6. Przedziały niezawodności

| Strength group | Reliability level, γ | Selective average, \bar{x} | Dispersion, D | Mean-square deviation, σ |
|----------------|-----------------------------|------------------------------|------------------|---------------------------------|
| S-135 | 0.005 | (0.45; 0.57) | (0.28; 0.28) | (0.194; 0.194) |
| G-105 | 0.005 | (0.55; 0.63) | (0.0148; 0.0148) | (0.141; 0.141) |

Statistical analysis of the location of defects that form along the length of a drill string

Because 81 DPs of strength group S-135 and 89 DPs of strength group G-105 were rejected at Ukrburgaz wells in 2018 and 2019 when wells were drilled to a depth (L_{max}) of 4000 to 6000 m, the assessment of potentially dangerous areas along the length of the DS is carried out in relative units, by using the parameter L_f/L_{max} (where L_f is the depth of destructive defects along the length of the DS and L_{max} is the maximum depth of drilling). To do this, we divided the relative depth of failure (L_f/L_{max}) into a number of intervals, with the most characteristic level of the formation of operational defects and, accordingly, the number of defects detected.

The resulting variation series is presented in Table 7. A frequency diagram (Figure 7) and a histogram (Figure 8) were built for the distribution.

To assess the number of distributions (Table 7), the characteristic indicators – such as selective average, mode and median – were determined (Table 8), and numerical (Table 9) and relative (Table 10) indicators of variation, type of distribution and degree of asymmetry were established (Table 11). An interval assessment of the centre of the general totality was carried out according to the data, and the confidence interval for the general average was determined.

Because $Ex/S_{Ex} < 3$, the deviation from the normal distribution for the cases under consideration is considered insignificant.

The interval estimation of the centre of the general totality was done as with section 2, and the confidence interval for the average value of reliability was calculated. The results of the calculations are provided in Table 12. The calculations were obtained at the level of reliability of $\gamma = 0.005$, which

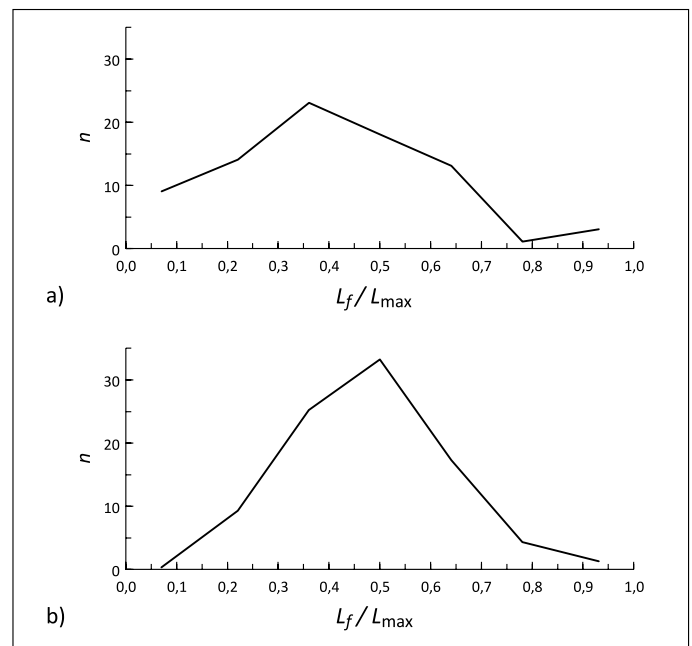


Figure 7. Frequency diagram: S-135 (a), G-105 (b)

Rysunek 7. Wykres częstotliwości: S-135 (a), G-105 (b)

Table 7. Number of failures at various lengths of drill strings, 2018–2019

Tabela 7. Dane o awariach przewodów wiertniczych o różnych długościach za lata 2018–2019

| Strength group | Length, L_f/L_{max} | | | | | | |
|----------------|-----------------------|-------------|-------------|-------------|-------------|-------------|-------------|
| | 0.000–0.143 | 0.143–0.286 | 0.286–0.429 | 0.429–0.571 | 0.571–0.715 | 0.715–0.858 | 0.858–1.000 |
| number, n | | | | | | | |
| S-135 | 9 | 14 | 23 | 18 | 13 | 1 | 3 |
| G-105 | 0 | 9 | 25 | 33 | 17 | 4 | 1 |

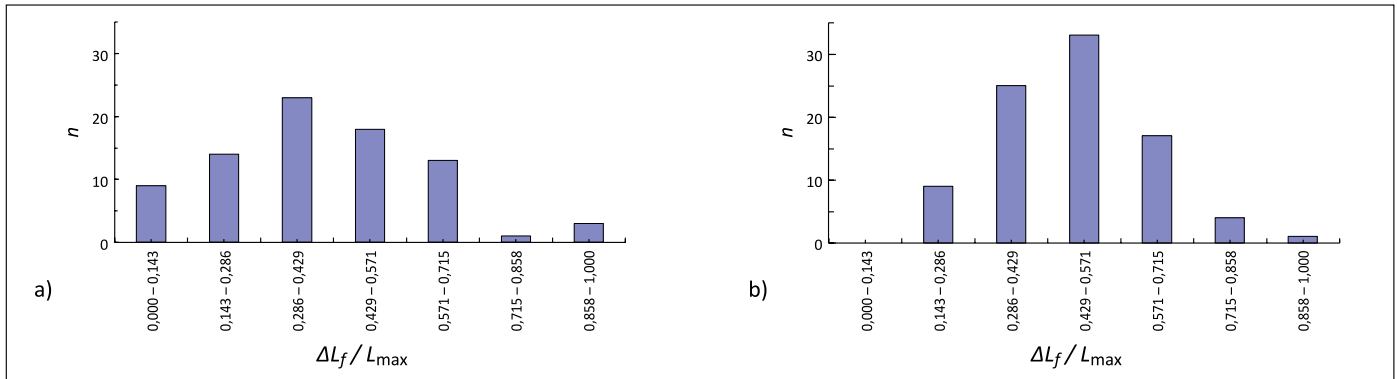


Figure 8. Histogram: S-135 (a), G-105 (b)

Rysunek 8. Histogram: S-135 (a), G-105 (b)

Table 8. Indicators that characterise the distribution series of the detected number of defects

Tabela 8. Wskaźniki charakteryzujące rozkłady serii wykrytej liczby defektów

| Strength group | Selective average | Mode | Median |
|----------------|-------------------|--------------|--------------|
| S-135 | $\bar{x} = 0.405$ | $Mo = 0.378$ | $Me = 0.395$ |
| G-105 | $\bar{x} = 0.476$ | $Mo = 0.476$ | $Me = 0.474$ |

Table 9. Numerical and absolute indicators of variation

Tabela 9. Liczbowe i bezwzględne wskaźniki zmienności

| Strength group | Range of variability | Mean linear deviation | Dispersion | Corrected dispersion | Standard deviation | Estimation of standard deviation |
|----------------|----------------------|-----------------------|--------------|----------------------|--------------------|----------------------------------|
| S-135 | $R = 1$ | $d = 0.167$ | $D = 0.0424$ | $S^2 = 0.0429$ | $\sigma = 0.206$ | $s = 0.207$ |
| G-105 | $R = 1$ | $d = 0.120$ | $D = 0.0023$ | $S^2 = 0.0233$ | $\sigma = 0.152$ | $s = 0.153$ |

Table 10. Relative indicators of variation

Tabela 10. Względne wskaźniki zmienności

| Strength group | Coefficient of variation | Relative linear deviation | Oscillation coefficient |
|----------------|--------------------------|---------------------------|-------------------------|
| | [%] | | |
| S-135 | $v = 50.81$ | $K_d = 41,24$ | $K_r = 246.94$ |
| G-105 | $v = 31.88$ | $K_d = 25.20$ | $K_r = 210.03$ |

Table 11. Indicators of the type of distribution and the degree of asymmetry

Tabela 11. Wskaźniki postaci rozkładu i stopnia asymetrii

| Strength group | Instantaneous asymmetry coefficient | Mean-square error of asymmetry coefficient | Pearson's asymmetry structural coefficient | Kurtosis indicator (peakedness) | Mean-square error of kurtosis coefficient | Materiality of kurtosis |
|----------------|-------------------------------------|--|--|---------------------------------|---|-------------------------|
| S-135 | $A_s = 0.348$ | $S_{A_s} = 0.612$ | $A_{sp} = 0.13^*$ | $Ex = -0,10^{**}$ | $S_{E_x} = 0.661$ | $Ex / S_{E_x} = -0.151$ |
| G-105 | $A_s = 0.286$ | $S_{A_s} = 0.612$ | $A_{sp} = 0.0014^*$ | $Ex = -0,0471^{**}$ | $S_{E_x} = 0.661$ | $Ex / S_{E_x} = -0.071$ |

* A positive sign indicates the presence of right-handed asymmetry

** A negative sign indicates a flat top distribution

Table 12. Reliability intervals

Tabela 12. Przedziały niezawodności

| Strength group | Reliability level, γ | Selective average, \bar{x} | Dispersion, D | Mean-square deviation, σ |
|----------------|-----------------------------|------------------------------|------------------|---------------------------------|
| S-135 | 0.005 | (0.34; 0.47) | (0.0317; 0.0317) | (0.206; 0.206) |
| G-105 | 0.005 | (0.43; 0.52) | (0.017; 0.017) | (0.152; 0.152) |

corresponds to the highest probability of an operational defect (Table 12).

It can be concluded from the results that during defectoscopy in DS pipes of strength group S-135, special attention should be paid to the DPs in the range of 0.34 to 0.47 along the relative length (L_f/L_{max}) of the string, as this area has the highest probability of an operational defect, but when diagnosing the DS pipes of strength group G-105, special attention should be paid to the interval from 0.43 to 0.52 of the relative length (L_f/L_{max}) of the string.

Statistical analysis of the formation of major defects depending on the duration of drilling

Table 13 presents data on DP destruction (Information Bulletin for 2018; Information Bulletin for 2019) obtained at the wells of Ukrburgaz in 2018 and 2019, according to intervals of service life (1000 hours each). After analysing the data for DPs of strength group S-135, three stages were

identified: Stage I – running-in (from launch to 2000 hours); Stage II – stable work (from 2000 to 7000 hours); and Stage III – accelerated destruction (7000 hours and longer). For DPs of strength group G-105, two stages were identified: Stage I – running-in and stable operation (from 0 to 6000 hours) and Stage II – accelerated destruction (6000 hours and longer).

To estimate the distribution intervals according to stages I–III for S-135 DPs and stages I–II for G-105 DPs (Table 13), the relevant characteristics were determined: selective mean, mode and median (Table 14); additionally, numerical (Table 15) and relative (Table 16) characteristics of variation and indicators for the type of distribution and the degree of asymmetry (Table 17) were established. According to the data, an interval assessment of the centre of the general totality was performed and the confidence interval for the general average for each of the stages was determined.

Because $Ex/S_{Ex} < 3$, the deviation from the normal distribution is considered insignificant.

The interval estimation of the centre of the general totality was done as with sections 2 and 3, and the confidence interval

Table 13. Data on DP failure depending on the duration of drilling, 2018–2019

Tabela 13. Dane o awarii rur płuczkowych w zależności od czasu trwania wiercenia dla lat 2018–2019

| Interval duration of operation, 1000 hrs | 0–1 | 1–2 | 2–3 | 3–4 | 4–5 | 5–6 | 6–7 | 7–8 | 8–9 | 9–10 | 10–11 | >11 |
|--|-----|-----|-----|-----|-----|-----|-----|-----|-----|------|-------|------|
| Average value | 0.5 | 1.5 | 2.5 | 3.5 | 4.5 | 5.5 | 6.5 | 7.5 | 8.5 | 9.5 | 10.5 | 11.5 |
| Stages of destruction S-135 | I | | | II | | | | III | | | | |
| Number, <i>n</i> | 21 | 9 | 2 | 5 | 2 | 1 | 3 | 6 | 10 | 8 | 4 | 10 |
| Stages of destruction G-105 | I | | | | | | II | | | | | |
| Number, <i>n</i> | 6 | 3 | 13 | 19 | 9 | 6 | 4 | 6 | 4 | 3 | 4 | 12 |

Table 14. Indicators that characterise the distribution of the number of defects detected

Tabela 14. Wskaźniki charakteryzujące rozkład liczby wykrytych defektów

| Stage of destruction | Selective average, \bar{x} | Mode, <i>Mo</i> | Median, <i>Me</i> |
|----------------------|------------------------------|-----------------|-------------------|
| S-135 | I | 800.000 | 636.36 |
| | II | 4346.154 | 3500.00 |
| | III | 9815.789 | 8667.00 |
| G-105 | I | 3214.286 | 3375.00 |
| | II | 9863.636 | 12200.00 |

Table 15. Numerical and absolute indicators of variation

Tabela 15. Liczbowe i bezwzględne wskaźniki zmienności

| Stage of destruction | Range of variability, <i>R</i> | Mean linear deviation, <i>d</i> | Dispersion, <i>D</i> | Corrected dispersion, S^2 | Mean-square deviation, σ | Estimation of mean-square deviation, <i>s</i> |
|----------------------|--------------------------------|---------------------------------|----------------------|-----------------------------|---------------------------------|---|
| S-135 | I | 2000 | 420.000 | 210000.00 | 217241.00 | 466.000 |
| | II | 5000 | 1218.935 | 1976331.36 | 2141024.19 | 1463.224 |
| | III | 7000 | 1556.787 | 3268698.06 | 3357050.80 | 1832.223 |
| G-105 | I | 6000 | 1097.000 | 1918367.35 | 1953247.75 | 1937.586 |
| | II | 8000 | 2071.625 | 5201101.93 | 5363636.36 | 2315.953 |

Table 16. Relative indicators of variation**Tabela 16.** Względne wskaźniki zmienności

| Stage of destruction | | Coefficient of variation, ν | Relative linear deviation, K_d | Oscillation coefficient, K |
|----------------------|-----|---------------------------------|----------------------------------|------------------------------|
| S-135 | I | 57.28 | 52.50 | 250.00 |
| | II | 32.35 | 28.05 | 115.04 |
| | III | 18.42 | 15.86 | 71.31 |
| G-105 | I | 43.09 | 34.13 | 186.67 |
| | II | 23.12 | 21.00 | 81.11 |

Table 17. Indicators of the type of distribution and the degree of asymmetry**Tabela 17.** Wskaźniki postaci rozkładu i stopnia asymetrii

| Stage of destruction | | Instantaneous asymmetry coefficient, A_s | Mean-square error of asymmetry coefficient, S_{A_s} | Pearson's asymmetry structural coefficient, A_{sp} | Kurtosis indicator (peakedness), Ex | Mean-square error of kurtosis coefficient, S_{Ex} | Materiality of kurtosis, Ex/S_{Ex} |
|----------------------|-----|--|---|--|---------------------------------------|---|--------------------------------------|
| S-135 | I | 0.873 | 0 | 0.36* | -1.24** | 0 | 0 |
| | II | 0.440 | 0.612 | 0.60* | -1.19** | 0.5 | -2.38 |
| | III | 0.430 | 0.612 | 0.64* | -1.22** | 0.5 | -2.38 |
| G-105 | I | -0.3270 | 0.617 | -0.12* | -0.36** | 0.597 | -0.603 |
| | II | -0.0532 | 0.617 | -1.02* | -1.55** | 0.597 | -2.597 |

* A negative sign indicates left asymmetry and a positive sign indicates right asymmetry

** A negative sign indicates a flat-top distribution

Table 18. Reliability intervals**Tabela 18.** Przedziały niezawodności

| Stage of destruction | | Reliability level, γ | Selective average, \bar{x} | Dispersion, D | Mean-square deviation, σ |
|----------------------|-----|-----------------------------|------------------------------|------------------------|---------------------------------|
| S-135 | I | 0.005 | (602; 998) | (133 195; 133 195) | (331; 587) |
| | II | 0.005 | (3348; 5344) | (1 016 254; 1 016 254) | (886; 1926) |
| | III | 0.005 | (8942; 10 584) | (2 007 832; 2 007 832) | (1364; 2225) |
| G-105 | I | 0.005 | (2692; 3736) | (1 363 525; 1 363 525) | (1125; 1645) |
| | II | 0.005 | (8744; 10983) | (3 128 285; 3 128 285) | (1688; 2876) |

of reliability for the average value of reliability was calculated. The results of the calculations are given in Table 18. According to the calculations at the level of reliability of $\gamma = 0.005$, which corresponds to the highest probability of an operational defect, determined, considering the duration of operation, time intervals of increased attention during defectoscopy of DS pipes.

It can be concluded from the results that during defectoscopy of DS pipes of strength group S-135, special attention should be paid to DPs, the service life of which is from 602 to 998 hours at the first stage, from 3348 to 5344 hours at the second stage and from 8942 to 10 584 hours at the third stage.

For DS pipes of strength group G-105, the stages demanding special attention are from 2692 to 3736 hours at the first stage and from 8744 to 10983 hours at the second stage, as in these periods there is the greatest probability of an inadmissible defect.

Conclusions

On the basis of statistical analysis of 81 DPs of strength group S-135 and 89 DPs of strength group G-105 which were rejected for drilling wells on the territory of the Dnipro-Donetsk gas and oil region in 2018 and 2019, it was found that during defectoscopy of DS pipes of strength group S-135 increased attention should be paid to the area of the pipe 0.45 m to 0.57 m from the end of the coupling or nipple, and while diagnosing DS pipes of strength group G-105, the area requiring close attention is from 0.55 m to 0.63 m.

In addition, considering the depth of drilling, increased attention during defectoscopy on DS pipes of strength group S-135 should be paid to the range of 0.34 to 0.47 m, along the relative length (L_p/L_{max}) of the string, because this area has the highest probability of an operational defect. When diagnosing DS pipes of strength group G-105, however, special attention

should be paid to the interval from 0.43 to 0.52 of the relative length (L_f/L_{max}) of the string.

It is also necessary to pay attention to the duration of DP operation, particularly when conducting defectoscopy of DS pipes of strength group S-135, special attention should be paid to DPs, the service life of which is from 602 to 998 hours at the first stage, from 3348 to 5344 hours at the second stage and at from 8942 to 10584 hours at the third stage. For DS pipes of strength group G-105, the stages demanding special attention are the time intervals of 2692 to 3736 hours at the first stage and from 8744 to 10983 hours at the second stage, as these periods have the highest probability of an inadmissible defect.

References

- Ahmed M.H., El-Zomor M.A., Khafagi S.M., El-Helaly M.A., 2020. Metallurgical failure analysis of twisted-off heavy weight drill-pipe. *Engineering Failure Analysis*, 112: 104531. DOI: 10.1016/j.engfailanal.2020.104531.
- Albdiry M.T., Almensory M.F., 2016. Failure analysis of drillstring in petroleum industry: A review. *Engineering Failure Analysis*, 65: 74–85. DOI:10.1016/j.engfailanal.2016.03.014.
- Bazaluk O., Velychkovych A., Ropyak L., Pashechko M., Pryhorovska T., Lozynskiy V., 2021. Influence of heavy weight drill pipe material and drill bit manufacturing errors on stress state of steel blades. *Energies*, 14(14): 4198. DOI: 10.3390/en14144198.
- Dalyak T.M., Shatskiy I.P., 2020. Interference of closable cracks and narrow slits in an elastic plate under bending. *Journal of the Serbian Society for Computational Mechanics*, 14(2): 51–68. DOI: 10.24874/jsscm.2020.14.02.04.
- Dmytrakh I.M., Syrotyuk A.M., Leshchak R.L., 2018. Specific features of the deformation and fracture of low-alloy steels in hydrogen-containing media: Influence of hydrogen concentration in the metal. *Materials Science*, 54(3): 295–308. DOI: 10.1007/s11003-018-0186-z.
- Guo L., Zeng Y., Huang J., Wang Z., Li J., Han X., Qian L., 2022. Fatigue optimization of rotary control head rubber core based on steady sealing. *Engineering Failure Analysis*, 132: 105935. DOI: 10.1016/j.engfailanal.2021.105935.
- Hrabov's'kyi R.S., 2009. Determination of the resource abilities of oil and gas pipelines working for a long time. *Materials Science*, 45(2): 309–317. DOI: 10.1007/s11003-009-9180-9.
- Information Bulletin for 2018 on accidents, complications and marriage at work during drilling in "UKRBURGAS" Drilling Department.
- Information Bulletin for 2019 on accidents, complications and marriage at work during drilling in "UKRBURGAS" Drilling Department.
- Kalbfleisch J.D., Prentice R.L., 2011. The Statistical Analysis of Failure Time Data. 2nd Edition. *John Wiley & Sons, Inc., New York*.
- Kryzhaniv's'kyi E.I., Hrabov's'kyi R.S., Fedorovych I.Y., Barna R.A., 2015. Evaluation of the Kinetics of Fracture of Elements of a Gas Pipeline After Operation. *Materials Science*, 51(1): 7–14. DOI: 10.1007/s11003-015-9804-1.
- Kryzhaniv's'kyi E.I., Hrabov's'kyi R.S., Mandryk O.M., 2013. Estimation of the serviceability of oil and gas pipelines after long-term operation according to the parameters of their defectiveness. *Materials Science*, 49(1): 117–123. DOI: 10.1007/s11003-013-9590-6.
- Kryzhaniv's'kyi E.I., Hrabov's'kyi R.S., Vytyaz' O.Y., 2018. Consideration of the geometry of corrosion-fatigue cracks in assessing residual life of long-term operation objects. *Materials Science*, 54(5): 647–655. DOI: 10.1007/s11003-019-00229-8.
- Kryzhaniv's'kyi E.I., Rudko V.P., Shats'kyi I.P., 2004. Estimation of admissible loads upon a pipeline in the zone of sliding ground. *Materials Science*, 40(4): 547–551. DOI: 10.1007/s11003-005-0076-z.
- Kryzhanivskiy Ye., Vytyaz O., Tyrlych V., Hrabovskyy R., Artym V., 2021. Evaluation of the conditions of drill pipes failure during tripping operations. *SOCAR Proceedings*, 1: 036–048. DOI: 10.5510/OGP20210100478.
- Liu R., Zhang T., Wu X., Wang C.H., 2004. Crack closure effect on stress intensity factors of an axially and a circumferentially cracked cylindrical shell. *International Journal of Fracture*, 125: 227–248. DOI: 10.1023/B:FRAC.0000022237.64448.b9.
- Liu Y., Li F., Xu X., Yang B., Lu C., 2011. Simulation technology in failure analysis of drill pipe. *SREE Conference on Engineering Modelling and Simulation (CEMS 2011)*. *Procedia Engineering*, 12: 236–241.
- Liu Y., Lian Z., Lin T., Shen Y., Zhang Q., 2016. A study on axial cracking failure of drill pipe body. *Engineering Failure Analysis*, 59: 434–443. DOI: 10.1016/j.engfailanal.2015.11.004.
- Lu S., Feng Y., Luo F., Qin C., Wang X., 2005. Failure analysis of IEU drill pipe wash out. *International Journal of Fatigue*, 27: 1360–1365.
- Lukin N., Moura R.T., Alves M., Brünig M., Driemeier L., 2020. Analysis of API S-135 steel drill pipe cutting process by blowout preventer. *Journal of Petroleum Science and Engineering*, 195: 107819. DOI: 10.1016/j.petrol.2020.107819.
- Moisyshyn V., Levchuk K., 2017. Investigation on releasing of a stuck drill string by means of a mechanical jar. *Oil & Gas Science and Technology – Revue d'IFP Energies nouvelles*, 72(5). DOI: 10.2516/ogst/2017024.
- Panasjuk V.V., Dmytrakh I.M., Toth L., Bilyi O.L., Syrotyuk A.M., 2014. A method for the assessment of the serviceability and fracture hazard for structural elements with cracklike defects. *Materials Science*, 49(5): 565–576. DOI: 10.1007/s11003-014-9650-6.
- Pryhorovska T., Ropyak L., 2019. Machining error influence on stress state of conical thread joint details. *IEEF 8th International Conference on Advanced Optoelectronics and Lasers, CAOL*: 493–497. DOI: 10.1109/CAOL46282.2019.9019544.
- Ropyak L.Ya., Pryhorovska T.O., Levchuk K.H., 2020. Analysis of materials and modern technologies for PDC drill bit manufacturing. *Progress in Physics of Metals*, 21(2): 274–301. DOI: 10.15407/ufm.21.02.274.
- Shats'kyi I.P., Dalyak T.M., 2002. Closure of cracks merged with slots in bent plates. *Materials Science*, 38(1): 24–33. DOI: 10.1023/A:1020164529724.
- Shats'kyi I.P., Makoviichuk M.V., 2009. Analysis of the limiting state of cylindrical shells with cracks with regard for the contact of crack lips. *Strength of Materials*, 41(5): 560–565. DOI: 10.1007/s11223-009-9166-8.
- Syrotyuk A.M., Dmytrakh I.M., 2014. Methods for the evaluation of fracture and strength of pipeline steels and structures under the action of working media. Part I. Influence of the corrosion factor. *Materials Science*, 50(3): 324–339. DOI: 10.1007/s11003-014-9724-5.
- Tutko T., Dubei O., Ropyak L., Vytvytskyi V., 2021. Determination of Radial Displacement Coefficient for Designing of Thread Joint of Thin-Walled Shells. *Advances in Design, Simulation, Manufacturing IV*: 153–162. DOI: 10.1007/978-3-030-77719-7_16.
- Tyrlych V., Moisyshyn V., 2019. Predicting remaining lifetime of drill pipes basing upon the fatigue crack kinetics within a pre-critical period. *Mining of Mineral Deposits*, 13(3): 127–133. DOI: 10.33271/mining13.03.127.

Velychkovych A.S., Andrusyak A.V., Pryhorovska T.O., Ropyak L.Y., 2019. Analytical model of oil pipeline overground transitions, laid in mountain areas. *Oil and Gas Science and Technology – Revue de IIFP*, 74(65): DOI: 10.2516/ogst/2019039.

Vytyaz O.Y., Hrabovskyy R.S., Artym V.I., Tyrlych V.V., 2020. Effect of geometry of internal crack-like defects on assessing trouble-free operation of long-term operated pipes of drill string. *Metallofizika i Noveishie Tekhnologii*, 42(12): 1715–1527. DOI: 10.15407/mfint.42.12.1715.

Zamani S.M., Hassanzadeh-Tabrizi S.A., Sharifi H., 2016. Failure analysis of drill pipe: A review. *Engineering Failure Analysis*, 59: 605–623. DOI: 10.1016/j.engfailanal.2015.10.012.

Zvirko O.I., Kryzhanivskiy E.I., Nykyforchyn H.M., Krechkovska H.V., 2021. Methods for the Evaluation of Corrosion-Hydrogen Degradation of Steels of Oil-and-Gas Pipelines. *Materials Science*, 56(5): 585–592. DOI: 10.1007/s11003-021-00468-8.



Oleg VYTYAZ, D.Sc.

Director of the Institute of Petroleum Engineering
Ivano-Frankivsk National Technical University
of Oil and Gas
15 Karpatska St., Ivano-Frankivsk, 76019, Ukraine
E-mail: o.vytyaz@gmail.com



Roman HRABOVSKIY, Prof., D.Sc.

Professor at the Department of Construction
and Civil Engineering
Ivano-Frankivsk National Technical University
of Oil and Gas
15 Karpatska St., Ivano-Frankivsk, 76019, Ukraine
E-mail: hrabovskyy.r@gmail.com



Yevstakhii KRYZHANIVSKIY, Prof., D.Sc.
Academician of the National Academy of Sciences
of Ukraine
Rector of the Ivano-Frankivsk National Technical
University of Oil and Gas
15 Karpatska St., Ivano-Frankivsk, 76019, Ukraine
E-mail: rector@nung.edu.ua



Volodymyr TYRLYCH, Ph.D.

Associate Professor at the Department
of Advanced Mathematics
Ivano-Frankivsk National Technical University
of Oil and Gas
15 Karpatska St., Ivano-Frankivsk, 76019, Ukraine
E-mail: turluch27@ukr.net